



저작자표시-비영리-변경금지 2.0 대한민국

이용자는 아래의 조건을 따르는 경우에 한하여 자유롭게

- 이 저작물을 복제, 배포, 전송, 전시, 공연 및 방송할 수 있습니다.

다음과 같은 조건을 따라야 합니다:



저작자표시. 귀하는 원저작자를 표시하여야 합니다.



비영리. 귀하는 이 저작물을 영리 목적으로 이용할 수 없습니다.



변경금지. 귀하는 이 저작물을 개작, 변형 또는 가공할 수 없습니다.

- 귀하는, 이 저작물의 재이용이나 배포의 경우, 이 저작물에 적용된 이용허락조건을 명확하게 나타내어야 합니다.
- 저작권자로부터 별도의 허가를 받으면 이러한 조건들은 적용되지 않습니다.

저작권법에 따른 이용자의 권리는 위의 내용에 의하여 영향을 받지 않습니다.

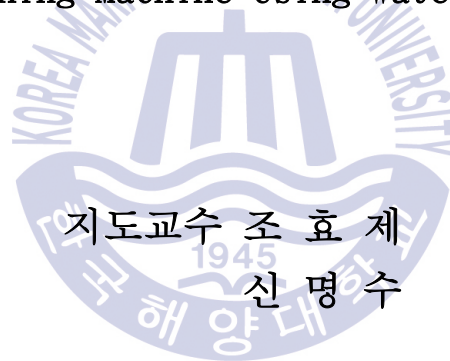
이것은 [이용허락규약\(Legal Code\)](#)을 이해하기 쉽게 요약한 것입니다.

[Disclaimer](#)

공학석사 학위논문

수조실험을 통한 해저지반 굴삭용
워터젯 장비의 성능평가에 관한 연구

Study on Performance Evaluation of Subsea Waterjet
Trenching Machine Using Water Tank



지도교수 조 효 제
신 명 수

2016년 2월

한국해양대학교 해양과학기술전문대학원

해양과학기술융합학과

나 경 원

본 논문을 나경원의 공학석사 학위논문으로 인준함.



위원장 이 승 재 (인)

위원 조 효 제 (인)

위원 신 명 수 (인)

2016년 2월

한국해양대학교 해양과학기술전문대학원

CONTENTS

List of Tables	iii
List of Figures	iv
Abstract	vi

CHAPTER 1 INTRODUCTION

1.1 Background	1
1.2 Advanced researches	6
1.3 Objective of the dissertation	9

CHAPTER 2 CLASSIFICATION & DESCRIPTION OF TRENCHING METHODS

2.1 Classification of trenching methods	10
2.1.1 Waterjet trenching method	11
2.1.2 Mechanical trenching method	12
2.1.3 Ploughing trenching method	13
2.2 Trenching depth corresponding to the seabed state	14
2.3 Description and principle of the ROV waterjet trencher	16
2.4 Configuration of waterjet injection pipe	17
2.5 Development trend of waterjet trenching machines	18

CHAPTER 3 EXPERIMENTAL METHODS & MODELS

3.1 Experimental equipments	20
-----------------------------------	----

3.1.1 Water pump	20
3.1.2 Towing carriage	21
3.1.3 Two-dimensional water tank	22
3.2 Simulation condition	23
3.3 Experimental models	25
3.4 Experimental methods and conditions	28
3.4.1 Experimental methods	28
3.4.2 Experimental conditions	30
CHAPTER 4 RESULTS & DISCUSSION	
4.1 Simulation results	32
4.2 Experimental results	37
4.2.1 Construction performance of Type I	37
4.2.2 Construction performance of Type II	41
4.3 Construction performance comparison	43
CHAPTER 5 CONCLUSION	47
References	49
감사의 글	51

List of Tables

Table 2.1 ROV waterjet trenchers currently in operation	19
Table 3.1 Simulation parameters	24
Table 3.2 Scale effect	29
Table 3.3 Nozzle variation of Type I	30
Table 3.4 Experimental conditions for Type I and Type II	31
Table 4.1 Simulation results of 6 nozzles	34
Table 4.2 Simulation results of 12 nozzles	35
Table 4.3 Simulation results of 18 nozzles	36



List of Figures

Fig. 1.1 Prospect of subsea flowlines	01
Fig. 1.2 Encased-type construction method	03
Fig. 1.3 ROV waterjet trencher	05
Fig. 1.4 Advanced experiment researches	08
Fig. 1.5 Diagram of research process	09
Fig. 2.1 Classification of trenching machines according to seabed condition ..	10
Fig. 2.2 Waterjet trenching method	11
Fig. 2.3 Mechanical cutter trenching method	12
Fig. 2.4 Ploughing trenching method	13
Fig. 2.5 Cross section of seabed ground after trenching	14
Fig. 2.6 Classifications of ROV waterjet trencher	16
Fig. 2.7 Waterjet injection pipe mounted on ROV trencher	17
Fig. 3.1 CR 15-6 pump	20
Fig. 3.2 CR 15-6 performance curve	20
Fig. 3.3 Towing carriage	21
Fig. 3.4 Two-dimensional water tank	22
Fig. 3.5 Front view of jetting-arm's nozzles arrangement	24
Fig. 3.6 Jetting arm type	26
Fig. 3.7 Backpipe type	27
Fig. 3.8 Schematic of the experimental method	28
Fig. 4.1 Simulation of 6 nozzles	34
Fig. 4.2 Simulation of 12 nozzles	35
Fig. 4.3 Simulation of 18 nozzles	36
Fig. 4.4 Snapshot of Type I	37
Fig. 4.5 Nozzle diameter vs. trenching depth	39
Fig. 4.6 Trenching depth vs. trenching speed by flow rate	40

Fig. 4.7 Snapshot of Type II 41
Fig. 4.8 Trenching depth vs. trenching speed by flow rate 42
Fig. 4.9 Trenching speed comparison in accordance with flow rate 45
Fig. 4.10 Trenching depth comparison in accordance with flow rate ... 46



수조실험을 통한 해저지반 굴삭용 워터젯 장비의 성능평가에 관한 연구

나 경 원

한국해양대학교 해양과학기술전문대학원

해양과학기술융합학과

요 약

최근 해양에너지 수요 증가와 더불어 국가 간 정보 전달의 목적으로 매년 수천 km의 파이프라인 및 케이블이 해저면에 설치되고 있으며, 이는 시공시 육지보다 열악한 해양 환경에 놓이게 된다. 그러므로 다양한 해양외력 환경에 노출되어 있는 해저케이블 및 해저파이프라인의 안정성을 유지하기 위해 해저지반을 굴삭하여 구조물을 매설하는 방식이 선호된다. 이때 해저지반 상태와 해상조건 등은 작업효율에 영향을 미치게 되며, 작업해역 또한 대수심으로 이동함에 따라 단시간에 효율적인 시공은 필수적이다.

본 연구는 해저지반 굴삭을 위해 ROV 트랜처에 장착되는 워터젯 굴삭기의 시공성능 추정에 관한 연구이다. 먼저 전산유체해석을 통해 노즐간의 거리와 노즐 분사각도를 고려하여 굴삭효율을 극대화할 수 있는 최적 노즐수량을 선정하여, 실제 운용중인 워터젯 굴삭장비에 적용시켜 1/6으로 축소 제작하였다. 실험은 다양한 파라미터를 적용하여 형태가 다른 워터젯 굴삭기와 최대 굴삭심도 및 최대 굴삭속도를 파악함으로써 효율적인 시공성능을

갖는 워터젯 굴삭기를 도출하였다. 실험결과를 바탕으로 실제 ROV 트랜처에 장착되어 운용중인 워터젯 굴삭장비와 비교·분석함으로써 워터젯 장비의 효율성을 확인하였다.

KEY WORDS: 굴삭장비, 워터젯 굴삭기, 굴삭로봇, 굴삭심도, 굴삭속도



CHAPTER 1

INTRODUCTION

1.1 Background

As world energy consumption is expected to increase every year, the installation of offshore wind farms and plants for the production of subsea crude oil and natural gas is a growing trend. Therefore, installation and construction of subsea cables and pipelines for transporting the produced energy has gradually increased. Subsea cables not only transport energy produced from offshore wind farms to onshore, but also serve as a means for worldwide information transmission. Seabed pipelines are also considered important because crude oil and natural gas extracted from the ocean are supplied to onshore through them.

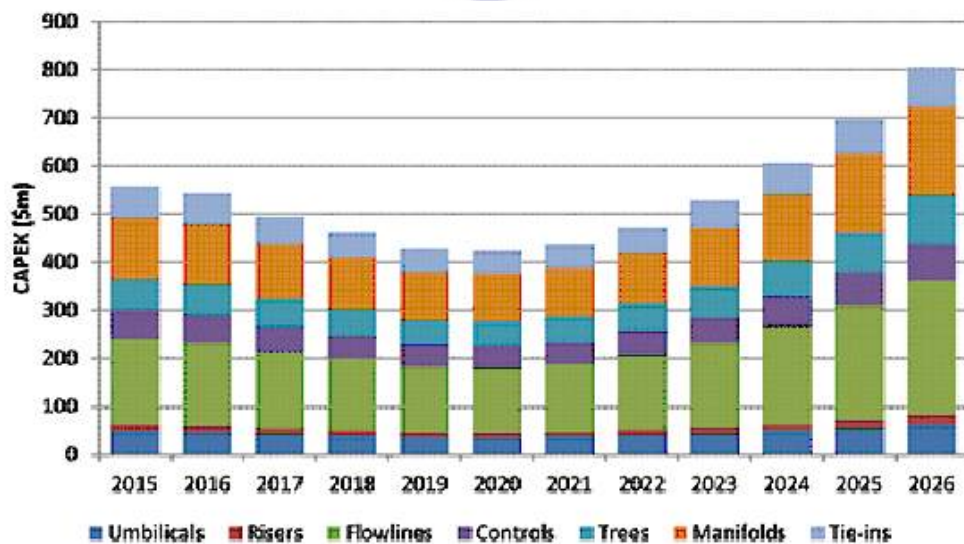
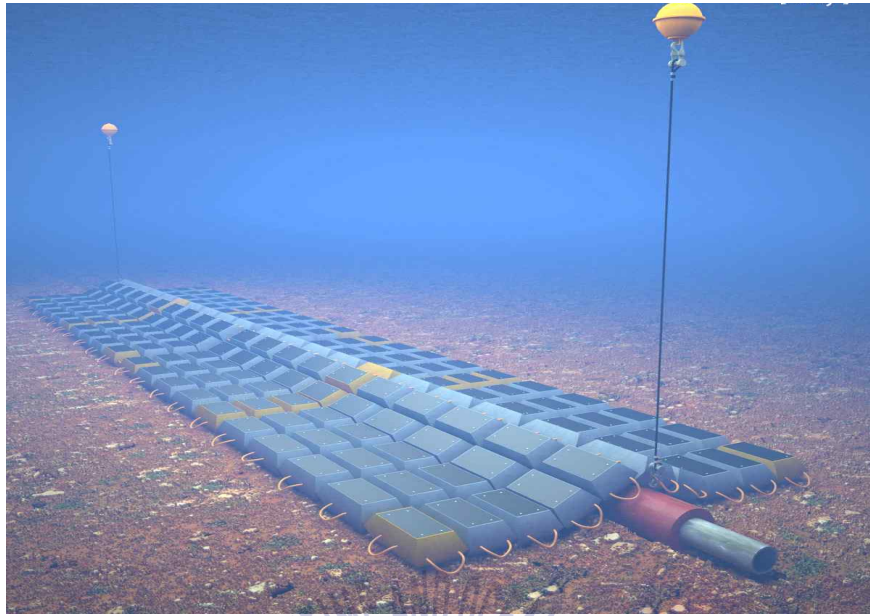


Fig. 1.1 Prospect of subsea flowlines

Unlike the ones in onshore, subsea cables and pipelines are exposed to various marine environments, including both natural elements such as waves, currents or subsea land slides, and artificial elements such as ship's anchors, trawl nets or discarded nets. The ocean resources should be unavoidably supplied under the poor environmental conditions. Thus, precise geotechnical surveys should be carried out for the seabed where cables or pipelines are to be buried and the essential requirements to safely supply the resources to onshore will be selection of appropriate protective construction methods for the facilities.

In general, the performance of construction methods are affected by soil characteristics and oceanographic conditions in the seabed where trenching and burial work is carried out. And the work efficiency could be difference depending on the seabed conditions. In the perspective of optimal construction performance, the seabed soil characteristics in the area where the facilities has been scheduled to be buried need to be closely analyzed by some test methods, such as a Standard Penetration Test (SPT) or a Cone Penetration Test (CPT). Furthermore, as possible working days in the ocean are usually three times shorter than those onshore, the work efficiency could be improved if the environmental conditions of the area scheduled were fully considered prior to the construction.

There are basically two protective construction methods for subsea cables and pipelines against marine environments: an encased-type and a burial-type. To prevent various damages from the poor environment, an encased-type construction method enable structural stability to be secured by using concrete mattress, gravel or rubble. However, some disadvantages of this method include instability involved in the construction, cost-inefficiency and requirement of continuous reinforcement work. And there is a risk of losing structures due to the external force by the extreme ocean environment.



(a) concrete mattress



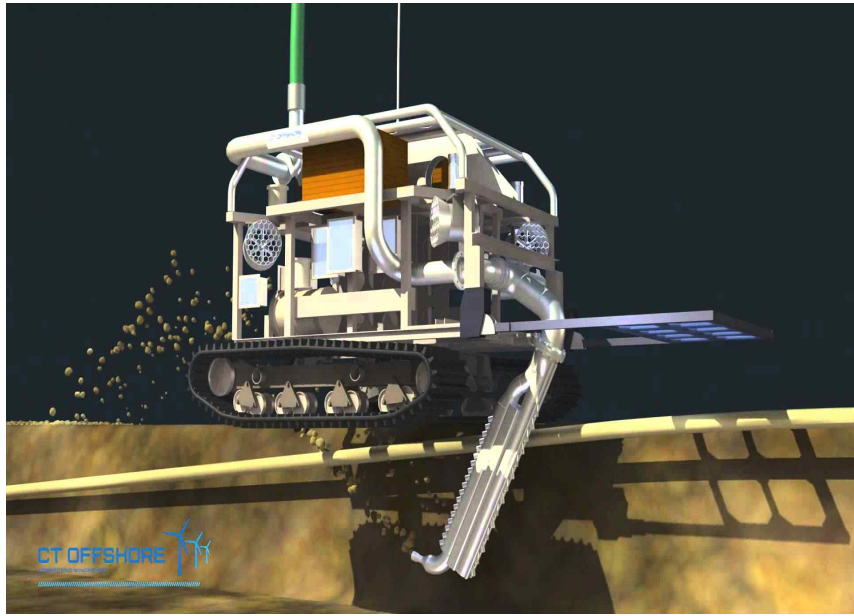
(b) concrete block

Fig. 1.2 Encased-type construction method

On the other hand, the burial-type construction method uses the way that cables or pipelines are buried with special machines for trenching the seabed soil and has a relatively simpler construction than an encased-type construction. Compared to an encased-type method, this method can provide more stability against marine external forces and is more economical as additional reinforcement work is usually not necessary.

Among the burying methods for pipelines and cables, a simultaneous lay and burial construction method has been mainly used, in which lay and burial work are performed at the same time by using trenching machines, such as ploughs. This method can shorten a construction period and stably bury cables and pipelines. However, its traction power increases as the depth of working waters becomes deeper, so that it is mainly used only in rivers and shallow seas. Because the burial-type has many advantages over the one an encased-type has and the burial areas tend to gradually move to deeper waters, the burial-type construction method with more structural stability is more preferred for its advantages in ease of the construction and in cost inefficiency.

In particular, as shown in Fig. 1.3, the PLIB (Post Lay Inspection and Burial) method has been widely used in which a waterjet machine is mounted to a ROV (Remotely Operated Underwater Vehicle) trencher, and cables and pipelines are laid and buried by spraying a large amount of water at high pressure, reducing the sediment density of the surrounding ground and directly removing or liquefying soil at the seabed.



(a) Above figure represent the waterjet trenching scene



(b) Actual waterjet trenching scene

Fig. 1.3 ROV waterjet trencher

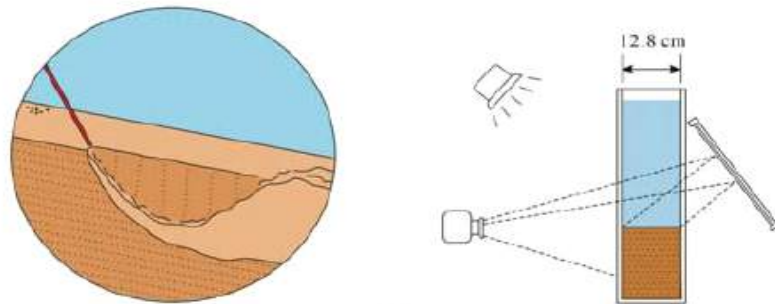
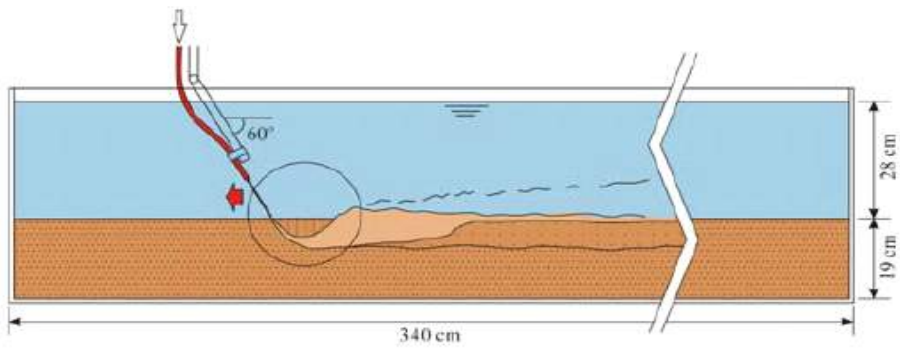
1.2 Advanced researches

The previous studies on the development and application principle of waterjet trenching methods have been mainly composed of papers which empirically approach through experimental results of phenomena occurring on the sand ground by applying waterjet machine in water.

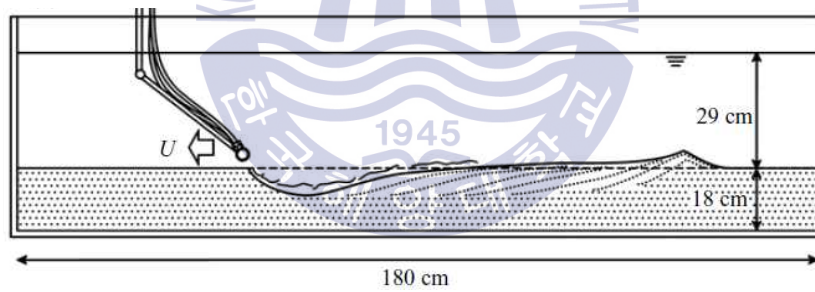
O'Donoghue et al. (2001) mounted waterjet machine vertically to a towing carriage. And then expressed in empirical formulas about trenching shapes corresponding to pressure sprayed from waterjet nozzles when a towing carriage moved along a water tank.

Su et al. (2007) and Berghe et al. (2008) used a single nozzle, Perng and Capart (2008) and Berghe et al. (2011) used multiple nozzle with waterjet machine, in a slope and analyzed and explained theoretically the floating and erosion phenomena of sand particles generated when moving them in water. Since these previous studies conducted experiments simply on phenomena occurring on the ground without burying waterjet machine under the ground. They were not able to simulate actual working environments in the subsea so that there are limitations in the reliability of the experiment results to estimate the performance and efficiency of the studied machines. Meanwhile, Adamson and Kolle (1996) mounted a waterjet machine having two nozzles to a towing carriage and moved them, while having it buried under the clayed ground. And proposed a nozzle structure for improving trenching performance.

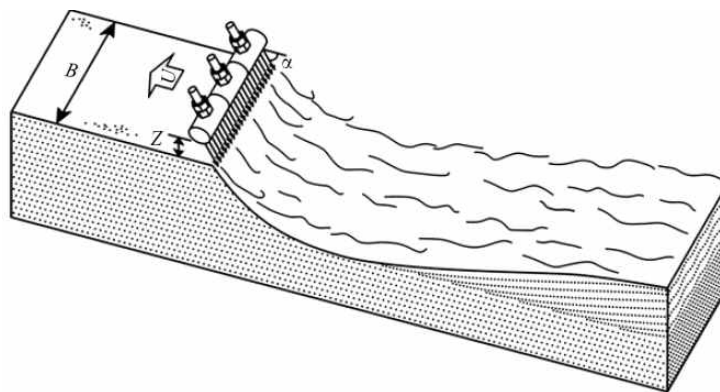
This study, however, is unique in that experimental research was conducted where waterjet machine having multiple nozzles were moved, while having them buried under the ground under a variety of marine working environment conditions.

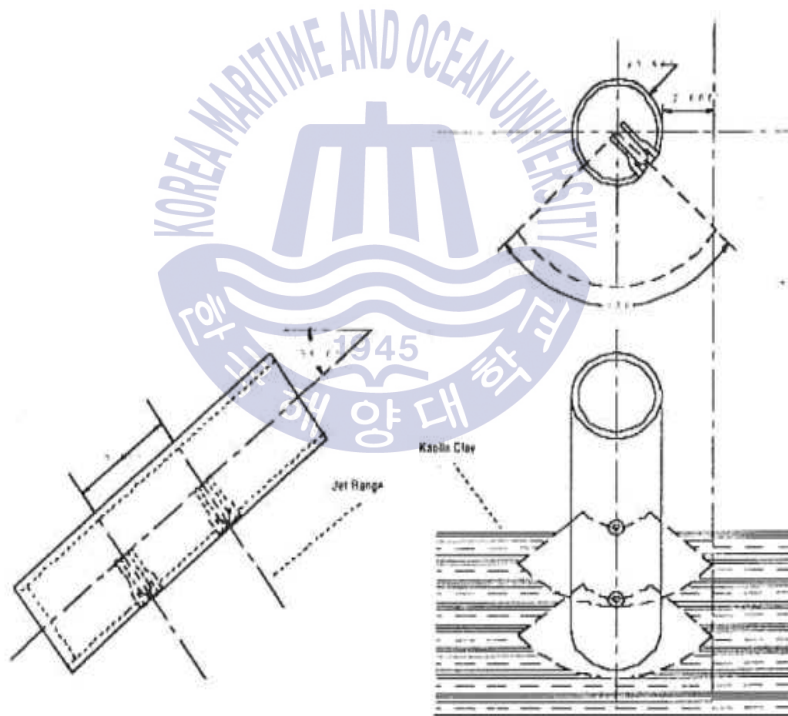
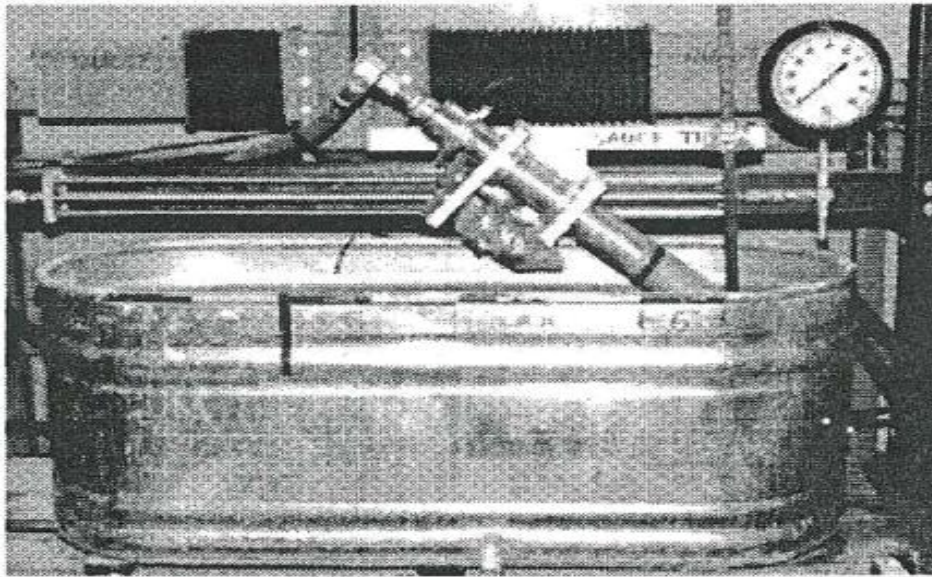


(a) Study of a single nozzle (Berghe et al., 2008)



(b) Study of multiple nozzles (Perng and Capart, 2008)





(c) Study of Adamson and Kolle(1996)

Fig. 1.4 Advanced experiment researches

1.3 Objective of the dissertation

As the installation areas of subsea cables and pipelines gradually move to deeper water and the construction scale gets bigger. Therefore, the role of divers tends to be replaced with an ROV trencher. For underwater construction work, various submarine construction machines are needed.

But this research was conducted only for a waterjet machine mounted to a ROV trencher. The configuration and distribution of nozzles of a waterjet machine are elements that directly affect its trenching depth and speed, and are closely related to construction performance and efficiency.

The research process conducted in this study is as shown in Fig. 1.5. To determine the nozzle numbers to be installed on a jetting arm for optimum construction performance, simulations were conducted using a computational fluid dynamics method. A waterjet arm type with an optimum number of nozzles and backpipe type machine was fabricated to the size of 1/6 of the actual one. The experiments were conducted with a nozzle diameter, a trenching speed, flow rate, and spray angle as its parameters to predict the maximum working efficiency. The experiments were conducted in a water tank, simulating the actual working area in subsea. Then the measured values were compared and analyzed with the construction performance of the actual waterjet trenching machines currently in operation.

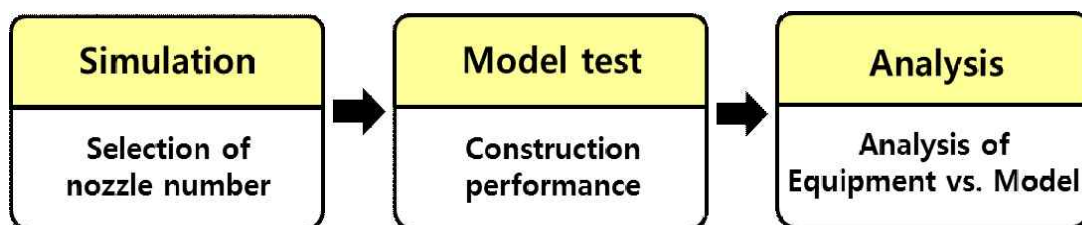


Fig. 1.5 Diagram of research process

CHAPTER 2

CLASSIFICATION & DESCRIPTION OF TRENCHING METHODS

2.1 Classification of trenching methods

The subsea trenching machines are divided into a waterjet type, a mechanical cutter type and a plough type depending on a trenching frame shape, which will be determined according to a geological condition, hardness and depth of the seabed ground. Fig. 2.1 shows in which the machines are classified according to the hardness of the seabed soil and geological conditions. The basic principles and features of these three trenching machines will be explained in the following chapter.

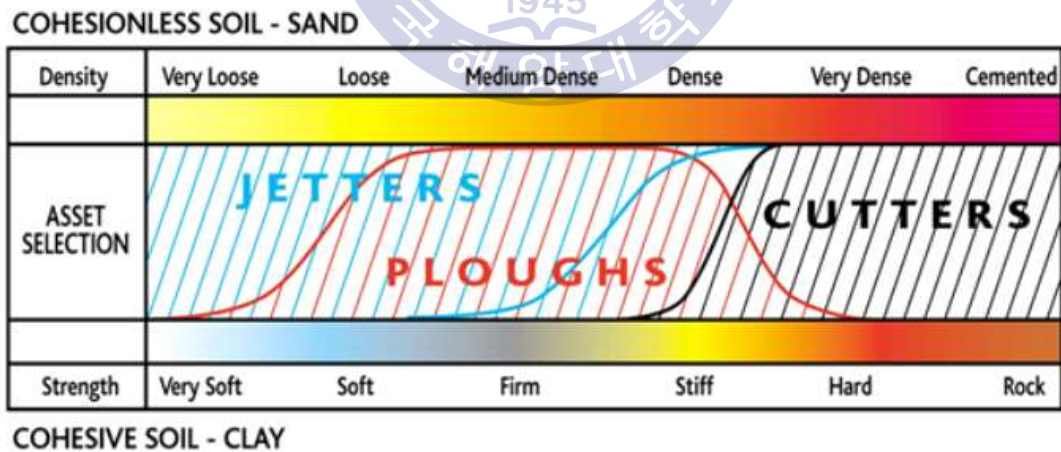


Fig. 2.1 Classification of trenching machines according to seabed condition

2.1.1 Waterjet trenching method

A waterjet trenching tool is currently the most common techniques in which spray pressure is generated by a motor or a power pump, and compressed air or water through nozzles at a high pressure of about 1MPa. It is sprayed into the front of the location where structures are to be buried, directly removing or liquefying the surrounding ground.

This method, it is important for the sides being trenched to be maintained at 20 ~ 30 degrees to prevent the collapse of those sides. And also its traction resistance is small, it is possible to work using a small tug boat and often utilized for re-burial after repair (Tateyama and Nishitani, 2000).



Fig. 2.2 Waterjet trenching method

2.1.2 Mechanical trenching method

A mechanical trenching tool is used when a waterjet method cannot make sufficient trenching effects where rocks bigger than gravel or hard sedimentary layers with very strong shear strength exist at the seabed. Usually, rock cutters, such as chain cutters or disk-shaped cutters are independently used by mounting them to a ship's hull. Basically, it is used for soft, cohesive soil, but not used for non-cohesive soil, such as sand. Due to the inefficiency that the ground soil is not removed immediately.

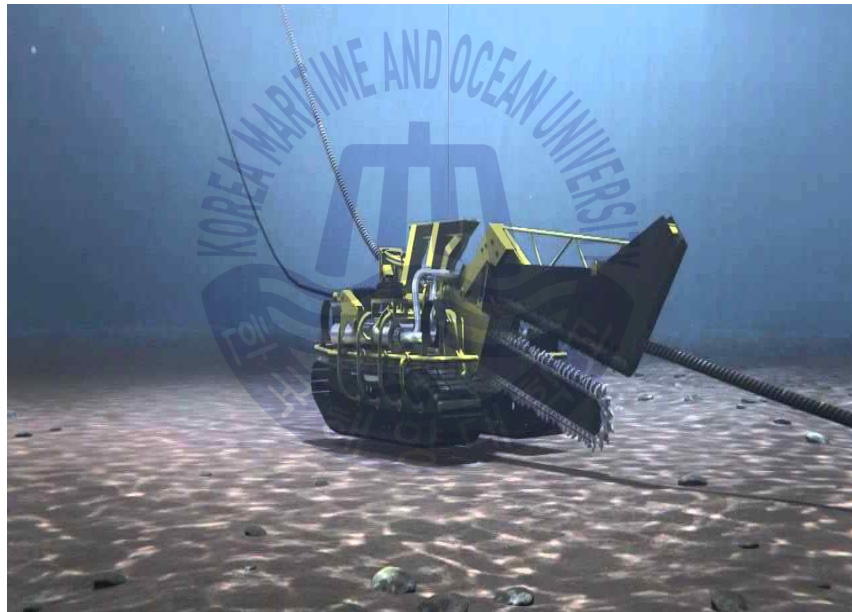


Fig. 2.3 Mechanical cutter trenching method

2.1.3 Ploughing trenching method

A ploughing trenching tool is used in which a ship with subsea cables on board tows a burial machine, and the vertical plough shares mounted to the bottom of the machine trench the seabed and bury cables or pipelines. This method has an advantage to minimize the construction period, by way of carrying out burying work at a desired depth and laying cables or pipelines on the seabed at the same time.

However, its use is limited, depending on the state of the seabed soil. It has been mainly used in rivers and shallow water because enormous towing force is needed in deepwater. This method is usually used where a pipe diameter is less than 30 inches, and a maximum trenching depth is 3.3m.

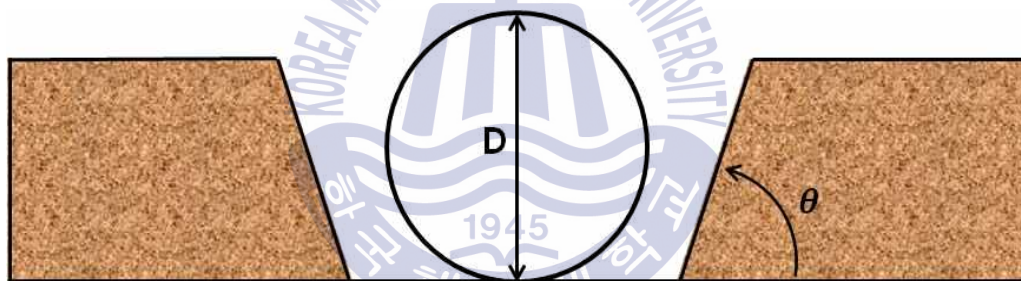


Fig. 2.4 Ploughing trenching method

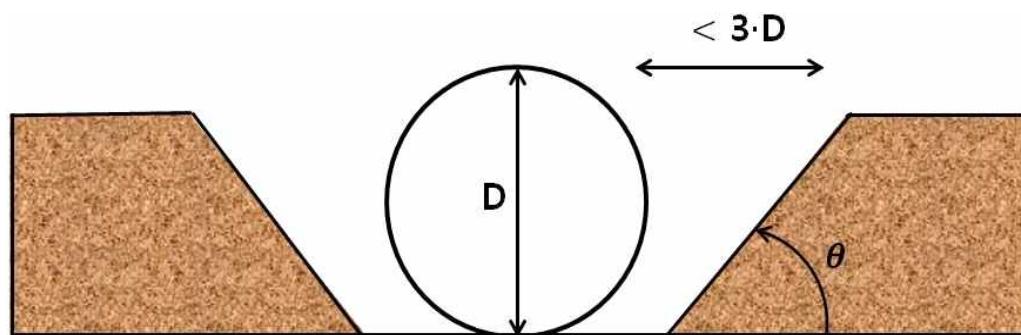
2.2 Trenching depth corresponding to the seabed state

Deepwater sedimentary layers, which have been formed over a long period of time, are composed of soft clay, silts or coarse grained soil. It has high adhesive properties. In general, in the cases of the seabed ground, there are hardened stratum at lower parts due to the upper layers' load. Even the seabed located in the same stratum and the same depth has different ground strengths (Seo et al., 2012).

As the seabed soil conditions determine the trenching speed, depth and cross sections, and slopes, etc., the elements that can affect construction performance shall be analyzed through a preliminary ground survey for pipelines or cables buried sections.



(a) cohesive soil seabed trenching



(b) Non-cohesive soil seabed trenching

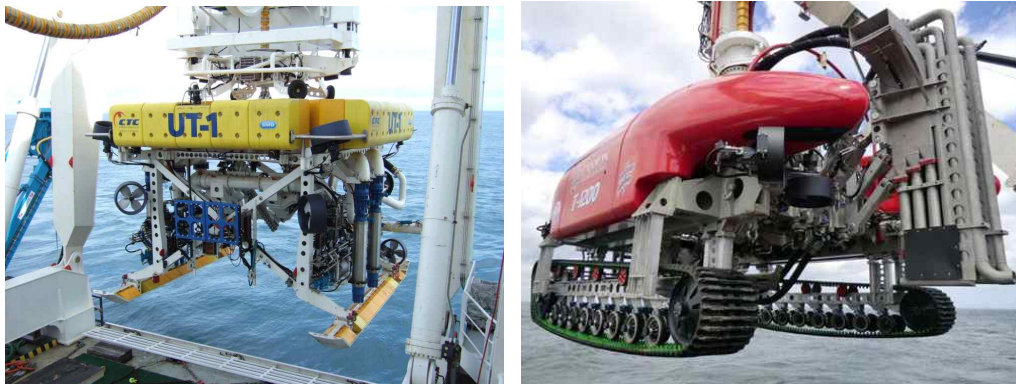
Fig. 2.5 Cross section of seabed ground after trenching

A waterjet trenching method is used for construction in both cohesive and non-cohesive ground except for the ground consisting of rocks. The viscosity of sediment affects the trenching speed and width.

Det Norske Veritas (2007) is suggested reasonable trenching width selection criteria for cables or pipelines burying work. To minimize the impact of external forces at the subsea when burying them, the trenching depth for optimum construction performance needs to be determined. The trenching width shall be less than $3 \cdot D$ when burying cables or pipelines, where D is the diameter (D) of a structure.

Fig. 2.5 (a) and (b) briefly show cross sections when a waterjet trencher is used both at the cohesive and non-cohesive soil. In the case of a cohesive soil seabed which contains a lot of silt and clay, its trenching slope tends to not easily collapse, and the trenching speed is slow even when applying high pressure waterjet sprays. On the other hand, in the case of a non-cohesive seabed which contains a relatively high amount of sandy soil, its trenching slope tends to easily collapse even at low spray pressure. Moreover, as the trenching speed increases, its work efficiency and construction performance tends to increase as well.

2.3 Description and principle of the ROV waterjet trencher



(a) Skid type

(b) Caterpillar track type

Fig. 2.6 Classifications of ROV waterjet trencher

A ROV trencher is a type of ROV-based underwater working robot. Mainly performs the burial and maintenance work of subsea cables or small diameter pipelines. The trenching work of a typical waterjet method is performed such that while a pair of waterjet machines mounted to the bottom of ROV is lowered down by a hydraulic cylinder, they trench the seabed using high pressure water and bury cables or pipelines (Li et al., 2014).

Driving methods of the ROV trencher have two different types, depending on a given work. One method is such that it works while swimming, driven by a propeller or sliding like a sled, on the seabed using skids at both of its lower sides. The other method is such that it works while traveling on the seabed driven by a caterpillar track. Fig. 2.6 (a) is show skid type based ROV and (b) is a caterpillar track type based ROV.

2.4 Configuration of waterjet injection pipe

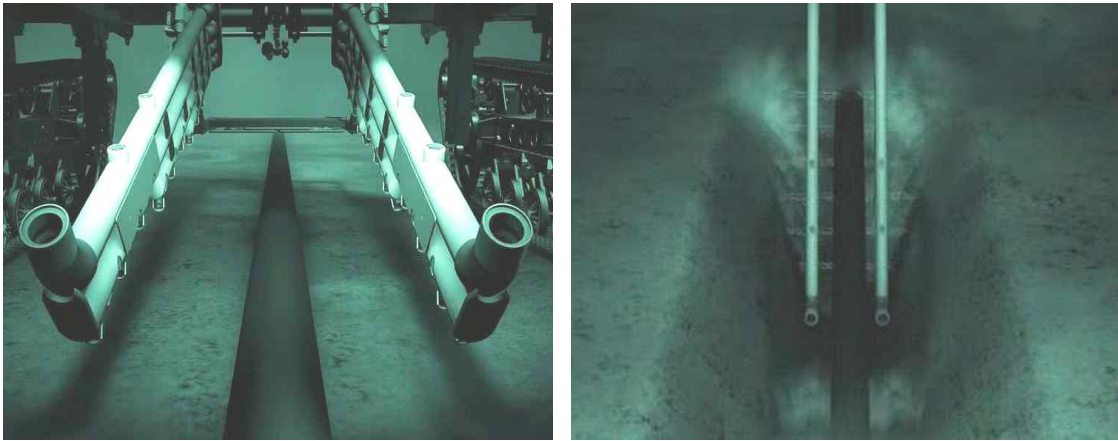


Fig. 2.7 Waterjet injection pipe mounted on ROV trencher

The space between the waterjet injection pipes, which are symmetrically mounted to both the lower sides of an ROV trencher, can be adjustable depending on the size of the outer diameter of buried objects.

At the earlier stages of trenching, waterjet machines with a single nozzle were used because the working depth was shallow. However, in recent years, as the working depth is getting deeper, high-pressure pumps have been developed and multiple nozzles are widely used for efficient construction. When using a single nozzle, it is advantageous in that its profile loss from a pump to a nozzle is small, thus resulting in better efficiency and being effective when trenching a narrow range of the seabed. Its controlling capability that can accurately trench the points is slightly inferior.

On the other hand, when multiple nozzles are used by a pump with the same capacity, a large profile loss occurs at each of the nozzles compared with a single nozzle, thus its efficiency drops. But, it is advantageous in that they can trench a wide area efficiently (Kozhevnikov, 2004).

The pumps for supplying water to waterjet injection pipes can be divided


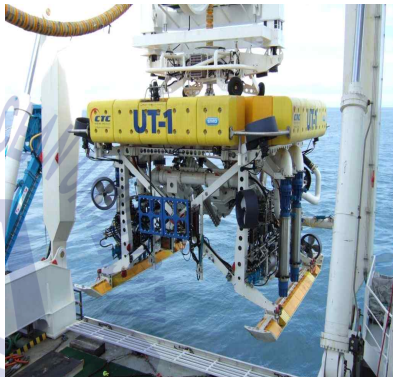
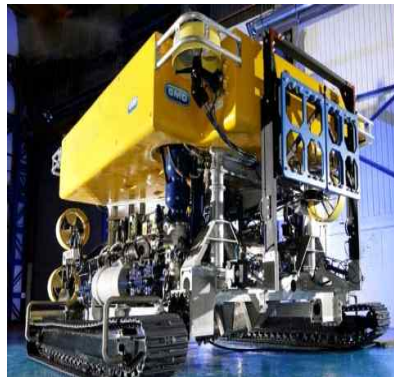
into a shipboard pump and an underwater pump according to its location. A shipboard pump supplies high pressure water from a dredger to a trenching machine through an umbilical line. But, it is using in deep water depth, its efficiency drops since the head loss of the pump increases. On the other hand, an underwater pump is mounted to a trenching machine, directly spraying surrounding water. Its efficiency is excellent, compared to a shipboard pump, as the concept of a head does not apply. Its actual size is large and its weight is heavy, so when it is mounted to a machine and used, it affects its placement and the center of gravity of the machine.

2.5 Development trend of waterjet trenching machines

The injection pipes of waterjet trenching machine in operation are generally divided into one-stage and multi-stage type. As the working depth gets deeper and the size of subsea construction gets bigger, it is expected that a multiple-stage type of two or more stages will be the mainstay in the future.

Table 2.1 summarizes the specifications of ROV trenchers currently used for pipeline or cable burying operations. The maximum depth which the three types of trenchers can trench is about 3m, and the trenching speeds vary depending on the specifications of the machines and the conditions of the seabed. Table 2.1 shows Canyon Helix Offshore's T-1200 from England; Deep Ocean's UT-1 from Norway; and Global Marine Systems Corporation's Q-1000 from England. On the bottom of table, the main specifications and working performance of each trencher are shown. In addition, the average daily operation time of the trenchers is 20 hours excluding the time for inspection, launching and recovery (Dansette and Robertson, 1994; Kim, 2006).

Table 2.1 ROV waterjet trenchers currently in operation

Specification		T-1200	UT-1	Q-1000
ROV trencher				
waterjetting system	Pump	375 * 3	375kW* 4	300kW*2
	Flow rate	1050 ~ 1800	4800	1000
	Pressure	8 ~ 16	7	8
Burial capabilities	Burial depth	3	0.75~3	3
	Burial speed	25 ~ 780	350~1000	400
	Soil condition	sand to soft clays		

CHAPTER 3

EXPERIMENTAL METHODS & MODELS

3.1 Experimental equipments

3.1.1 Water pump

A pump produces spraying water streams which play a role of actual trenching tools and is one of the parts through which the capacity of waterjet can be estimated. The pump used in this experiment is a CR 15-6 water pump from Grundfos Company. Its revolution speed is 3,529 rpm, its rated flow rate is 20.5m³/h and its rated lift is 98.5m.



Fig. 3.1 CR 15-6 pump

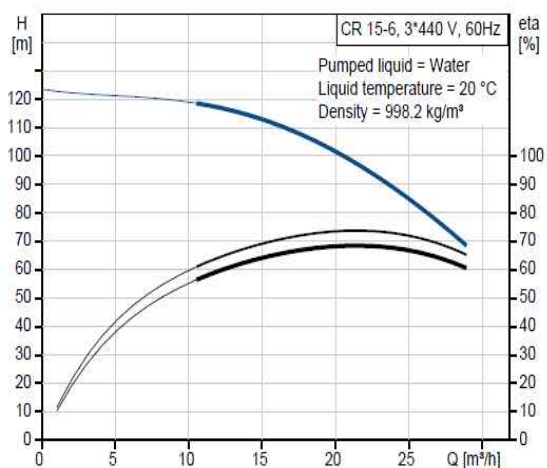


Fig. 3.2 CR 15-6 performance curve

3.1.2 Towing carriage

A towing carriage travels on the straight lines of X, Y and Z axis and oscillates in a direction of . It is operated by a rack and pinion system that allows it to travel along x-axis at a minimum speed of 0.11m/s to a maximum 0.33m/s. The positive and negative acceleration $0.5\text{m}^2/\text{s}$; and a traveling distance approximately 18m. The experiments were conducted with a waterjet trencher mounted to a towing carriage.



Fig. 3.3 Towing carriage

3.1.3 Two-dimensional water tank

The experiments were conducted, using a marine engineering water tank whose dimensions are $2.5\text{ m} \times 1\text{ m} \times 1.3\text{ m}$ ($L \times H \times W$). The tank belongs to the Ocean System Engineering Laboratory (OSEL) of Korea Maritime and Ocean University. An internal water tank where actual work can be simulated was assembled in aluminum frames whose size is $2.5\text{ m} \times 1\text{ m} \times 0.5\text{ m}$ ($L \times H \times W$).



(a) Inner tank



(b) Inner tank mounted on ocean engineering tank

Fig. 3.4 Two-dimensional water tank

3.2 Simulation condition

For simulations, flow field analysis was performed under a total of 6 cases using ANSYS CFX version 14.0 as shown in Table 3.1. In order to verify the validity of the turbulence model contained in the governing equation, a k-epsilon model was basically applied. Two jetting heads are designated as an inlet area for water to inflow. The area where nozzles are mounted, and shooting the water is designated as an outlet area.

The hydrostatic pressure in the water under the simulation conditions is the same in each case. The output condition of the nozzles was set at atmospheric pressure, assuming that there is no pressure from the outside. The flow rate applied to the simulations was selected considering the pump's performance used in the model experiments.

In order to determine the optimum numbers of nozzles through simulation analysis, only the forward direction nozzles are taken into account. The back-wash nozzles to remove the remaining sediment were not taken into account. In addition, as a condition for calculating the optimum numbers of nozzles, the flow velocity distribution of the water sprayed from the nozzles should be uniform. In addition, the interferences between the water spray from the nozzles were modeled such that they shall be minimized.

Fig. 3.5 shows the arrangement of the front parts of the nozzles of the jetting-arms used in simulations. Each nozzle was arranged to spray water to be crossed by 5 degrees to the left and right within a range that structures are not damaged. Under these arrangements, it is possible to make a wider trenching width and gentle slopes compared with nozzles spraying water at a right angle. So that it can reduce a risk of collapse of trenching slopes and improve the reliability of construction.

Table 3.1 Simulation parameters

Nozzle diameter [mm]	Flow rate [m ³ /h]	Forward direction nozzle number [A]	Total case
3	3.0 / 4.2	6 / 12 / 18	6



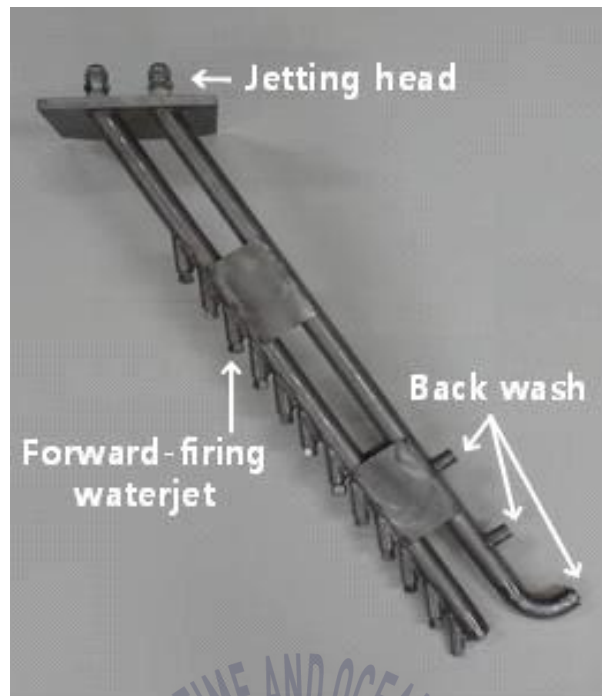
Fig. 3.5 Front view of jetting arm's nozzles arrangement

3.3 Experimental models

Two types of waterjet machines to be used in the experiments whose sizes are reduced to 1/6 of the actual ones as shown Fig. 3.6 is a jetting-arm type; and Fig. 3.7 is a back-pipe type, which are named Type I and Type II herein, respectively.

Type I is composed of forward-firing waterjet nozzles and back-wash nozzles. The forward-firing waterjet nozzles are used to trench the ground in a traveling direction. The back-wash nozzles are fabricated to balance with the forward-firing waterjet nozzles and removes soil which has been trenched (Adamson and Kollé, 1996). The forward-firing waterjet nozzles trench the ground, fabricated to be inclined 5 degree to the right and left, respectively. Two jetting heads are supplied water from a high-pressure hose and supply it to the back-wash nozzles and jetting nozzles.

Type II has only downward-firing waterjet nozzles towards the ground. It has a disadvantage in that it has no nozzles having a back-wash function, so that it cannot blow liquefied soil backwards. Thus, in order to compensate for this disadvantage, it uses nozzles with much larger diameters than Type I. And also four jetting heads are supplied water from a high pressure hose and supply it to the downward nozzles.

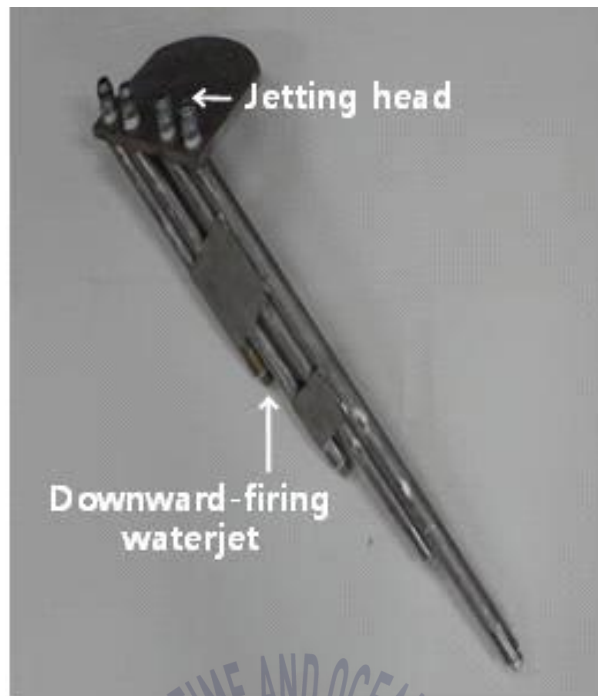


(a) Side view



(b) Front view

Fig.3.6 Jetting arm type



(a) Side view



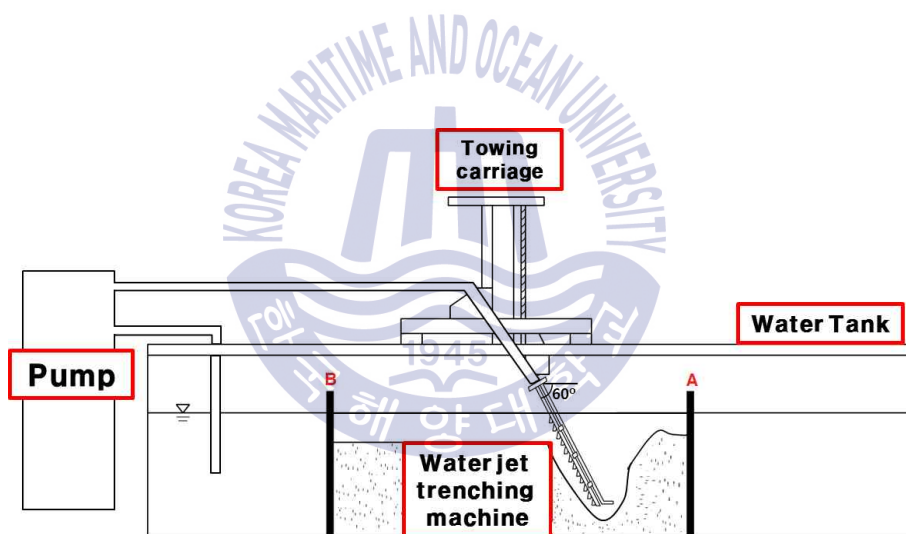
(b) Front view

Fig. 3.7 Backpipe type

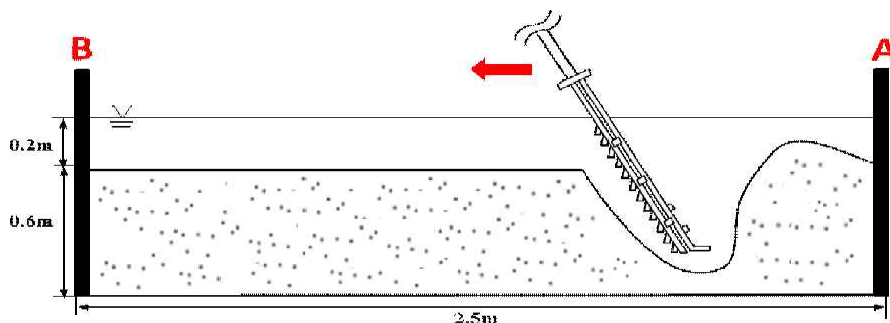
3.4 Experimental methods and conditions

3.4.1 Experimental methods

Fig. 3.8 is a schematic diagram showing the experimental environments. The average diameter of the sand particles which are made up of the ground is 0.012cm. In the case of sediment, the binding force between particles varies depending on its immersion duration. Thus, each experiment proceeded after soil has been stabilized at the same time interval of 30 minutes. A waterjet machine for the experiment, is made of stainless steel. A towing carriage with a waterjet machine mounted moves in the direction of A to B at a minimum speed of 0.11 m/s to a maximum 0.33 m/s.



(a) Configuration of equipment



(b) Scene of experiments

Fig. 3.8 Schematic of the experimental method

To converse its prototype into a model for small-scale laboratory experiments, a geometrical scale factor of 6 was assumed as shown in Table 3.2. Reducing the size of sand particles is very difficult applying scale factor. Even though it can be achieved geometric similarity, roughness, void ration and pore pressure that compose ground become different (Kang, 2015).

Also, the power of the pump is applied to formular (3.4) in Table 3.2, the calculated value is smaller than the minimum value to be operated pump. Thus, a commercial pump meeting the flow rate and pressure was used without a scale-down.

Table 3.2 Scale effect

Quantity	Model	Prototype	Equivalent value of the scale
Trench depth		L_p	$\frac{L_p}{L_m} SF = 6 \quad \dots\dots (3.1)$
Flow rate	Q_m	Q_p	$\frac{Q_p}{Q_m} = \frac{L_p^2 V_p}{L_m^2 V_m} = SF^{2.5} \quad \dots\dots (3.2)$
Water pressure	p_m	p_p	$\frac{p_p}{p_m} = \frac{V_p^2}{V_m^2} = SF \quad \dots\dots (3.3)$
Jetting power	P_m	P_p	$\frac{P_p}{P_m} = \frac{p_p Q_p}{p_m Q_m} = SF^{3.5} \quad \dots\dots (3.4)$
Progress rate of trencher or Water velocity through nozzle	V_m	V_p	$\frac{V_p}{V_m} = \frac{g L_p}{g L_m} = SF^{0.5} \quad \dots\dots (3.5)$

3.4.2 Experimental conditions

The experiments were conducted with three different nozzles diameters under the same condition of trenching speed and flow rate as shown in Table 3.3. The nozzle's diameter showing the greatest trenching depth was selected for Type I .

In order to measure the trenching depth by Type I with the selected nozzle, its experiment parameters put the trenching speeds and flow rate as shown in Table 3.4. In the case of Type II, its variables put the trenching speed and nozzle angle at the same flow rate of 3.4 m³/h.

Table 3.3 Nozzle variation of Type I

Variable Type	Nozzle angle [°]	Flow rate [m ³ /h]	Trenching velocity [m/s]	Nozzle diameter [mm]
I	90	4.2	0.11	3
				4
				5

Table 3.4 Experimental conditions for Type I and Type II

Type	Trenching velocity [m/s]	Flow rate [m ³ /h]	Nozzle angle [°]
I	0.11	3.0	90
		3.4	
		3.8	
		4.2	
	0.22	3.0	
		3.4	
		3.8	
		4.2	
	0.33	3.0	
		3.4	
		3.8	
		4.2	
II	0.11	3.4	60
			75
	0.22		60
			75
	0.33		60
			75

CHAPTER 4

RESULTS & DISCUSSION

4.1 Simulation results

The simulations were conducted as follows, the diameter of all nozzles was set to 3 mm. Under the three conditions of the different nozzle number 6, 12 and 18 pieces, the experiments were conducted by applying two flow rates 3 m³/h and 4.2 m³/h. Having analyzed the simulation results on all six conditions, the water flow rate and velocity through those nozzles tend to decrease rapidly as they get closer to the ground.

Fig. 4.1 shows the case where 6 nozzles were used. The flow rate from the first nozzle at the top was not enough to reach the ground. When only the remaining five nozzles are used for trenching, the construction performance will deteriorate as the trenching range becomes narrow. Thus ensuring the target depth will be difficult as well.

In the case of Fig. 4.3, have relatively more number of nozzles than the others. But the flow rate and velocity from the nozzles decrease rapidly as they get closer to the ground. Thus, its trenching performance will be inefficient since it is difficult to ensure sufficient trenching depth. In addition, it is predicted that the trenching efficiency is low because it takes relatively more trenching time, compared with Fig. 4.1 and Fig. 4.2. It was also found that there was reduction in the flow velocity due to interference in the vicinity of the nozzles even so in some nozzles without such interference.

However, in the case of Fig. 4.2 where 12 nozzles were used, the flow rate

and velocity showed generally uniform patterns except the first nozzles at the top. There was also no interference between nozzles. Thus, it is determined to demonstrate excellent work efficiency and optimal construction performance.

The reason not to exclude the first nozzle in this study was that if there is no first nozzle, the second one will show a similar pattern. As the second nozzle substantially trenches the ground, the first nozzle is necessary even though it has a lower flow rate. On the basis of the results of the simulations, the optimal number of nozzles was determined to be 12 piece. The reason that their spray patterns and rates are not uniform is due to the influence of turbulent flow and the fluid viscosity in the pipelines.



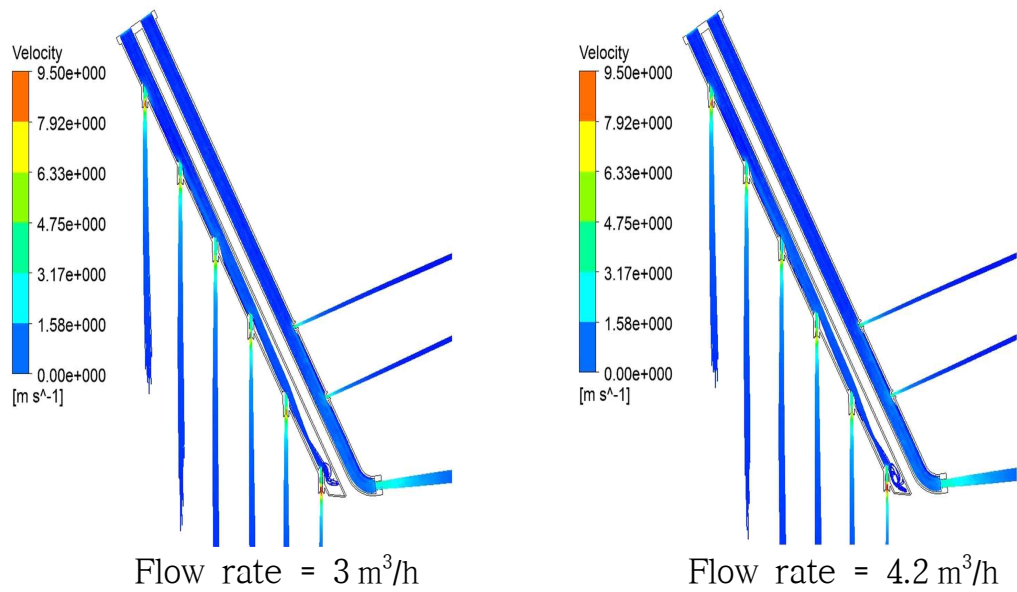


Fig. 4.1 Simulation of 6 nozzles

Table 4.1 Simulation results of 6 nozzles

Flow rate 3 m ³ /h			Flow rate 4.2 m ³ /h		
Nozzle no.	Flow velocity [m/s]	Flow ₃ rate [m ³ /h]	Nozzle no.	Flow velocity [m/s]	Flow ₃ rate [m ³ /h]
1	9.188	0.2334	1	12.37	0.3148
2	9.276	0.2360	2	12.62	0.3211
3	9.375	0.2386	3	13.61	0.3462
4	9.372	0.2385	4	14.21	0.3616
5	9.288	0.2364	5	14.124	0.3594
6	9.302	0.2367	6	14.496	0.3688

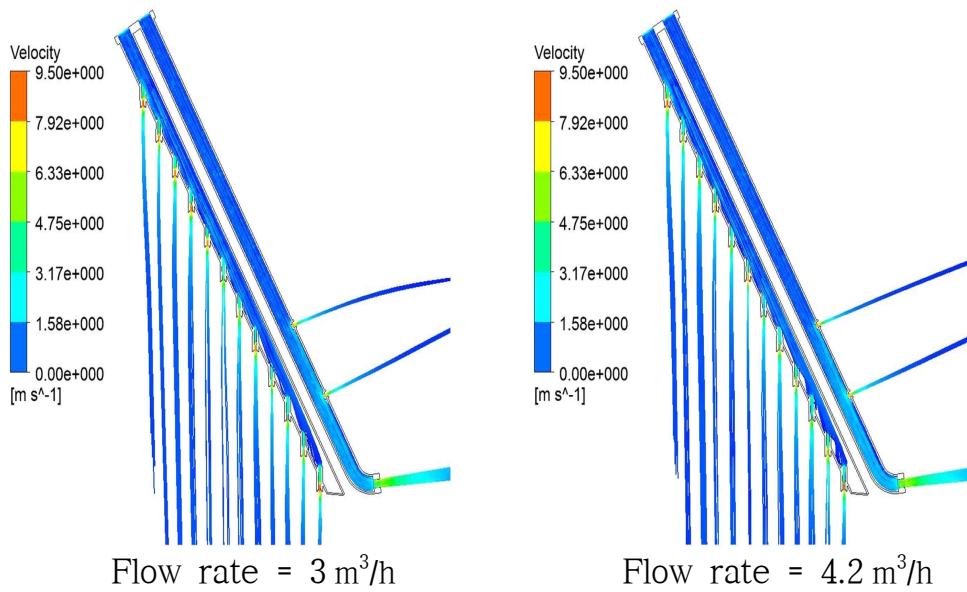


Fig. 4.2 Simulation of 12 nozzles

Table 4.2 Simulation results of 12 nozzles

Nozzle no.	Flow rate 3 m ³ /h		Nozzle no.	Flow rate 4.2 m ³ /h	
	Flow velocity [m/s]	Flow ₃ rate [m ³ /h]		Flow velocity [m/s]	Flow ₃ rate [m ³ /h]
1	4.851	0.1234	1	6.531	0.1662
2	5.117	0.1302	2	6.851	0.1743
3	5.191	0.1321	3	6.893	0.1754
4	5.191	0.1321	4	6.864	0.1747
5	5.023	0.1278	5	6.745	0.1718
6	4.954	0.1261	6	6.793	0.1729
7	4.923	0.1253	7	6.721	0.1710
8	5.077	0.1292	8	6.986	0.1778
9	4.993	0.1271	9	6.855	0.1744
10	5.073	0.1291	10	6.749	0.1717
11	5.0142	0.1276	11	6.829	0.1738
12	5.0130	0.1276	12	6.865	0.1747

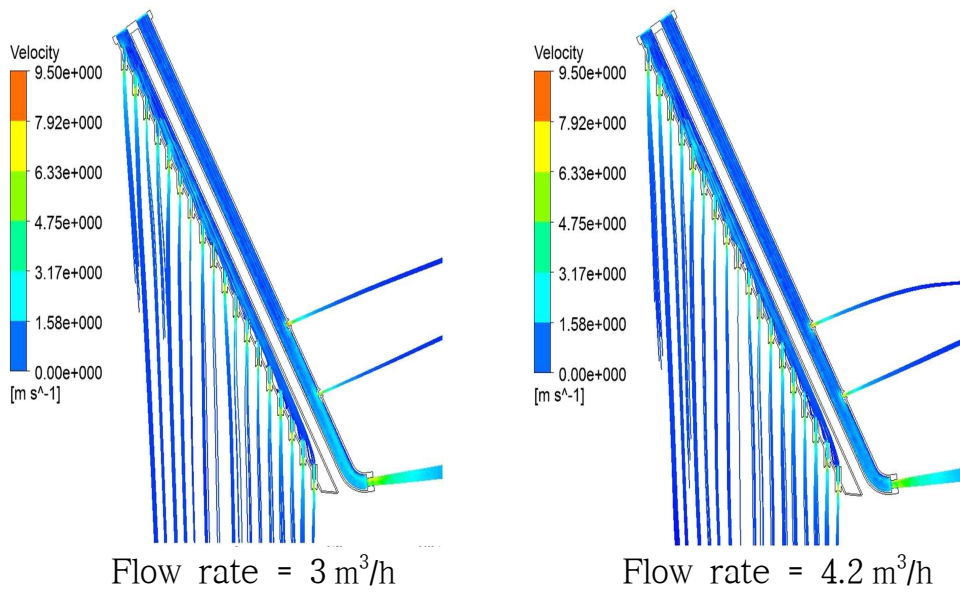


Fig. 4.3 Simulation of 18 nozzles

Table 4.3 Simulation results of 18 nozzles

Flow rate 3 m ³ /h			Flow rate 4.2 m ³ /h		
Nozzle no.	Flow velocity [m/s]	Flow ₃ rate [m ³ / h]	Nozzle no.	Flow velocity [m/s]	Flow ₃ rate [m ³ / h]
1	3.514	0.0894	1	4.618	0.1175
2	3.674	0.0935	2	4.550	0.1158
3	2.912	0.0741	3	4.025	0.1024
4	1.905	0.0485	4	4.560	0.0914
5	3.493	0.0889	5	4.371	0.1004
6	3.459	0.0670	6	4.048	0.1030
7	2.632	0.0880	7	3.946	0.1112
8	3.357	0.0854	8	3.780	0.0962
9	3.312	0.0733	9	2.846	0.0724
10	3.337	0.0849	10	3.591	0.1161
11	2.880	0.0845	11	3.547	0.0903
12	3.392	0.0863	12	4.730	0.1204
13	3.407	0.0867	13	4.703	0.1197
14	3.356	0.0854	14	4.795	0.1220
15	3.433	0.0874	15	4.460	0.1135
16	3.033	0.0772	16	4.170	0.1061
17	3.486	0.0887	17	4.689	0.1193
18	3.363	0.0856	18	4.257	0.1083

4.2 Experimental results

4.2.1 Construction performance of Type I



Fig. 4.4 Snapshot of Type I

The experimental scenes of Type I is given in Fig. 4.4. As the results of calculating the average values over repeated experiments by applying three nozzles with different diameters, the average trenching depths of 0.465 m, 0.372 m and 0.354 m were identified from the nozzle diameters of 3 mm, 4 mm and 5 mm, respectively.

The result is shown in Fig. 4.5. Since its spray pressure decreases as the nozzle diameter increases under the same flow rate condition. The 3 mm diameter nozzle was determined to be the optimum nozzle which is capable of maximizing trenching efficiency.

As can be seen from Fig. 4.6, the maximum trenching depth of Type I was measured under the flow rate of $4.2 \text{ m}^3/\text{h}$ and the trenching speed of 0.11 m/s . With respect to the flow rate of $3.0 \text{ m}^3/\text{h}$ and $3.4 \text{ m}^3/\text{h}$, there was difficulty in measuring a reliable trenching depth under experimental conditions with faster trenching speed than 0.11 m/s . Equally, at flow rate of $3.8 \text{ m}^3/\text{h}$ and trenching speed of 0.33 m/s , it is difficult to measure the trenching depth. Thus, the

shallow trenching depth was measured when it have the lower the flow rate and the faster the trenching speed. In order to ensure a certain level of trenching depth required in actual working sea area, it was found that at least $3.0 \text{ m}^3/\text{h}$ of a flow rate and 0.11m/s of a trenching speed are necessary.



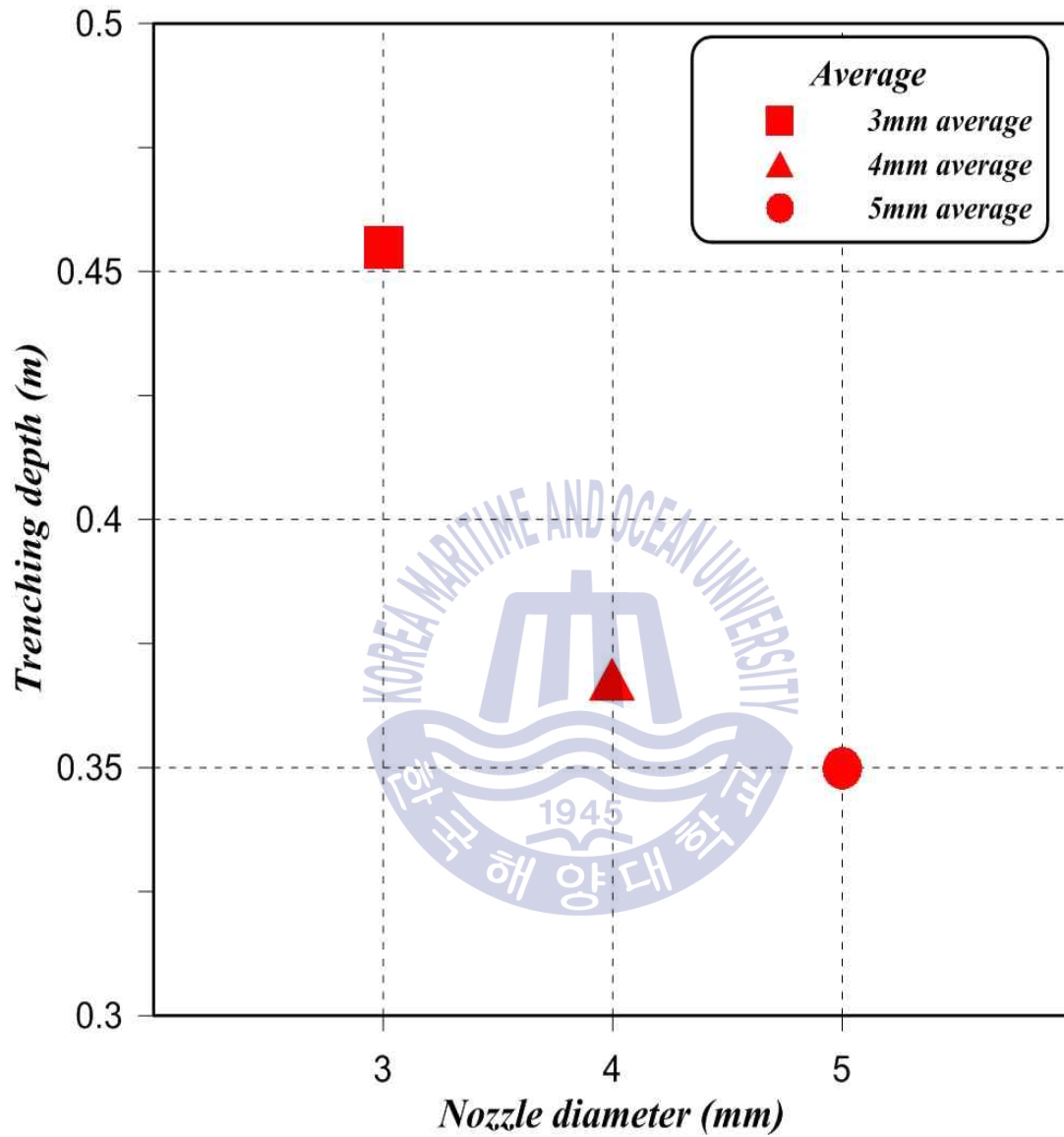


Fig. 4.5 Nozzle diameter vs. trenching depth

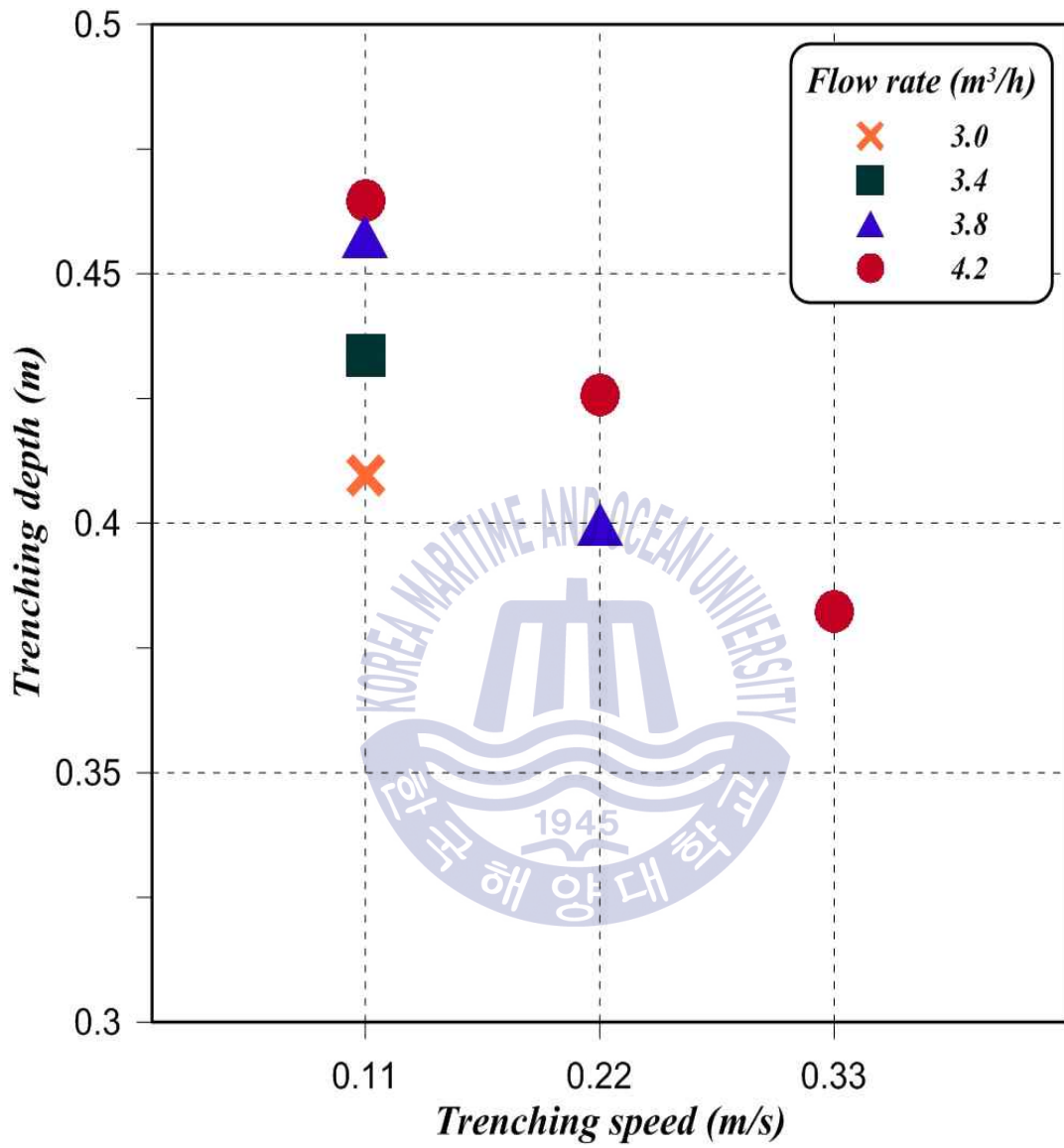


Fig. 4.6 Trenching depth vs. trenching speed by flow rate

4.2.2 Construction performance of Type II



Fig. 4.7 Snapshot of Type II

Fig. 4.7 is presented experimental scenes of Type II. It was determined to be insufficient to advance at a flow rate of $3.0 \text{ m}^3/\text{h}$ and at a flow rate of $3.8 \text{ m}^3/\text{h}$ or more excluded from analysis because of the lack of reliability in measured trenching depths due to the seabed disturbance.

Fig. 4.8 is a graph of trenching depths according to the changes in nozzle angles and trenching speeds of Type II as shown in Table 3.4. As a result, the trenching depths of 0.455 m, 0.351 m and 0.321 m were measured at the trenching speeds of 0.11 m/s, 0.22 m/s and 0.33 m/s, respectively, with a nozzle angle of 75 degree.

On the other hand, the trenching depth of 0.389 m was measured at the trenching speed of 0.11 m/s with a nozzle angle of 60 degree. However, there was difficulty measuring any significant trenching depths from the engineering perspective at a faster trenching speed than 0.11 m/s.

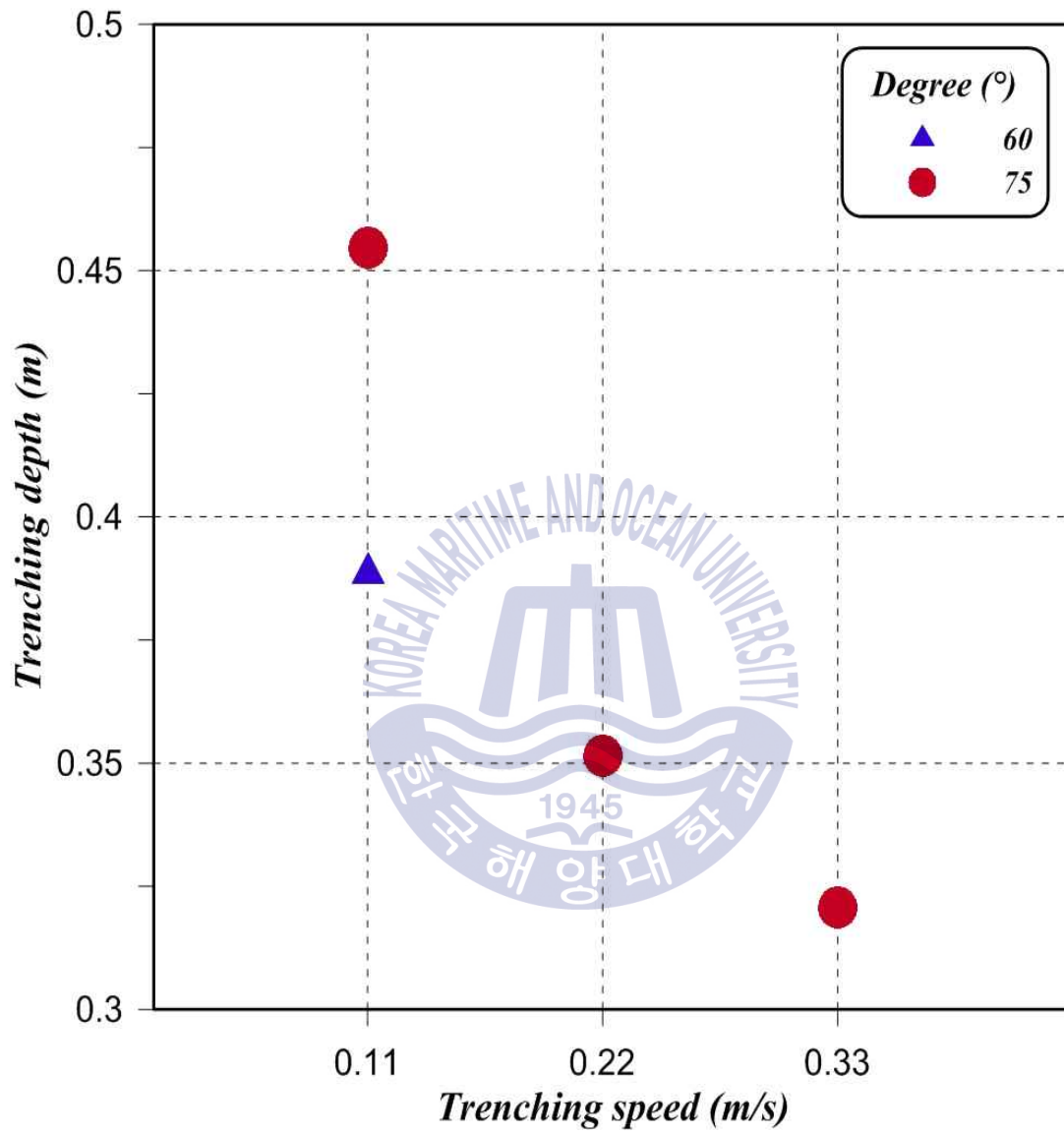


Fig. 4.8 Trenching depth vs. trenching speed by flow rate

4.3 Construction performance comparison

Fig. 4.9 and Fig. 4.10 are graphs comparing the results of having applied its scale factor 6 to the measurement obtained through model experiments with the actual construction performance of machines in operation in Table 2.1.

Fig. 4.9 is presented the comparison and analysis of the actual trenching speed of trenchers currently in operation with the measurement values obtained from experiments. A model fabricated with 12 nozzles which were selected through the analysis of the previous simulation results. When converting the trenching speed of the waterjet machine used in the experiments into an actual speed using (3.5) in Table 3.2. It was 970 m/h similar to that of UT-1, but significantly higher than those of T-1200 and Q-1000. Although the flow rate used in the experiments was 370 m³/h using (3.2) about 30% when compared with the flow rate of 1,200 m³/h of UT-1. The trenching speed applied to the experiments was about 970 m³/h very close to the maximum trenching speed of 1,000 m/h of UT-1. Moreover, although the waterjet machine used in the experiments has a relatively low flow rate compared to those of the trenchers presented in Table 2.1, it has a superior trenching speed when the same flow rate is applied.

Fig. 4.10 is a graph analyzing the trenching depths of trenchers currently in operation and those obtained through experiments based on flow rates. As a result of the experiments, the maximum trenching depth using (3.1) was measured 2.78 m. It is very similar to the maximum depth of 3 m. When comparing the results of the model experiments with the major construction performance of waterjet machines in Table 2.1, it is found that the model applied to the experiments has a superior ability for trenching depths when compared with those of trenchers based on the same flow rate. Therefore, it is estimated to have superior construction performance when operated in actual waters. In addition, the performance of the first nozzle used in the experiments has been demonstrated to be similar to that of the simulation.

Thus, a review might be necessary in the future according to the change in the position of the first nozzle.



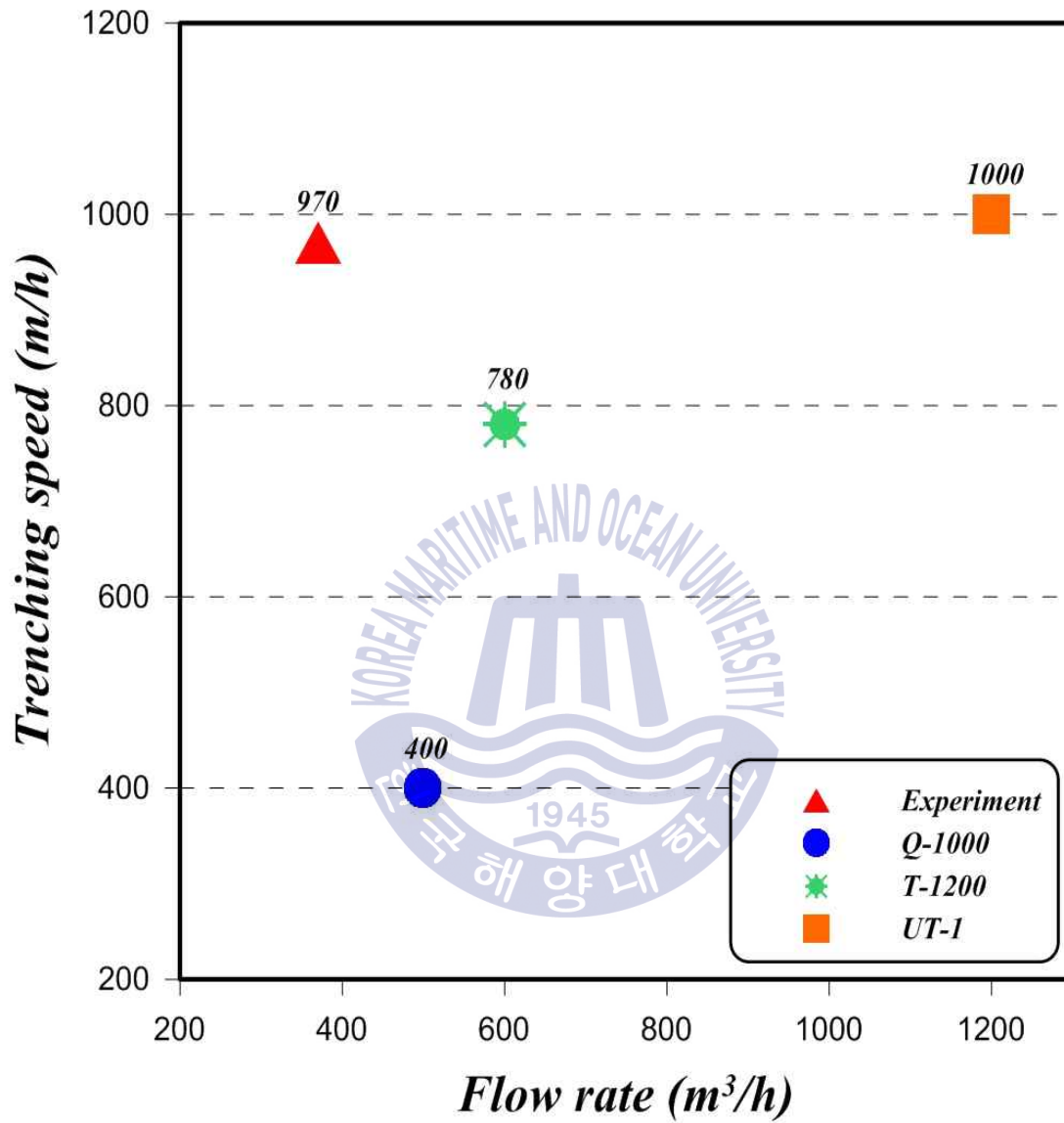


Fig. 4.9 Trenching speed comparison in accordance with flow rate

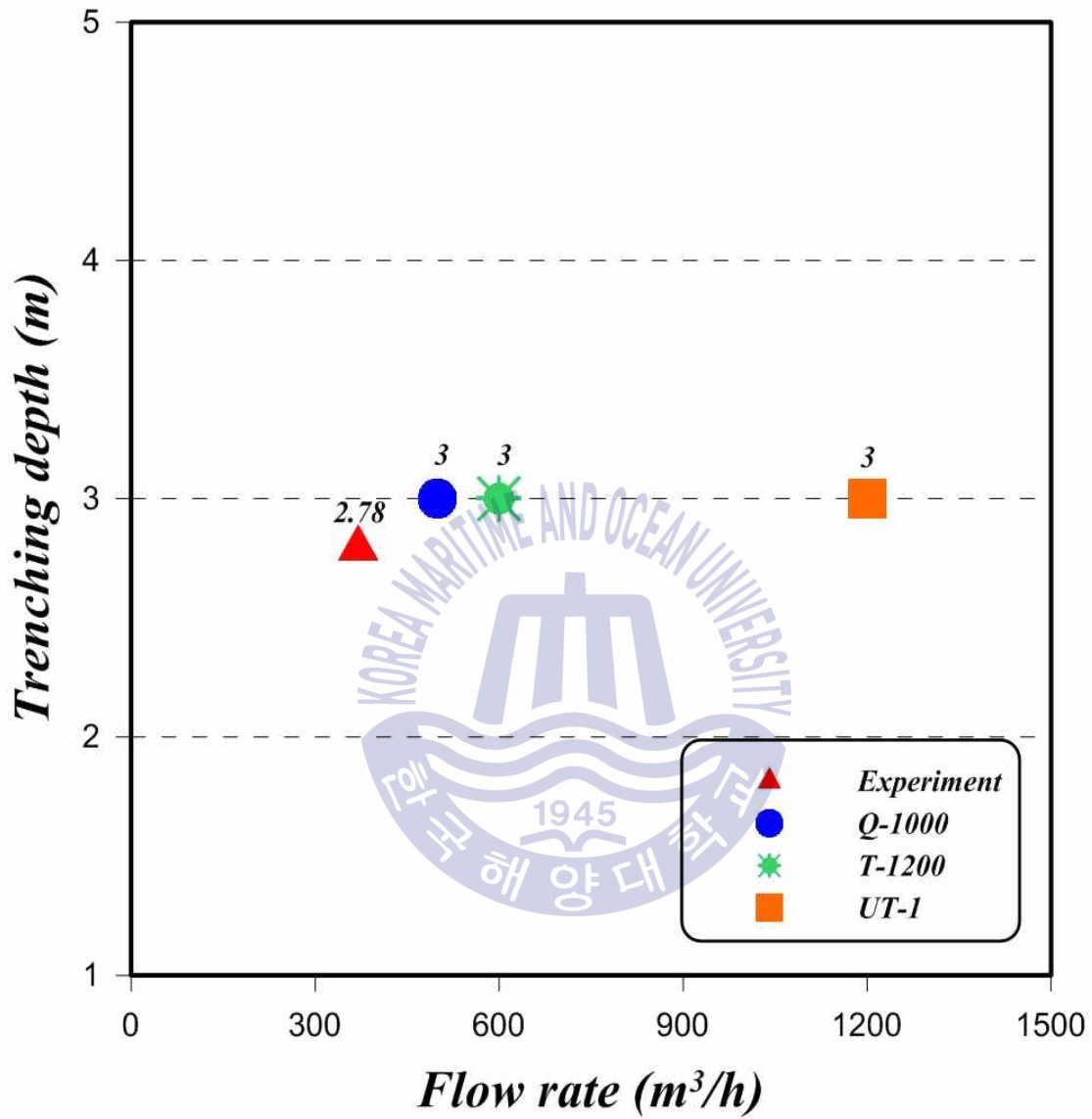


Fig. 4.10 Trenching depth comparison in accordance with flow rate

CHAPTER 5

CONCLUSION

This study has been conducted to estimate the construction performance of the waterjet machine mounted to an ROV trencher, it is used to lay and bury subsea cables and pipelines under the seabed. The number of nozzles with which the optimal working efficiency and construction performance can be demonstrated was selected through simulation. Based on the results, model experiments were conducted by fabricating a model into 1/6 of the actual size of a waterjet machine. Consequently, the following conclusions have been obtained by measuring the maximum trenching depth and speed through experiments and comparing them with those of the machines currently in operation:

- (1) As a result of simulations to determine the optimal number of nozzles for a waterjet machine, it is found that when having 12 nozzles, their mutual interference was small. And the flow rate and velocity from the nozzles was uniform, showing the most efficient construction performance.
- (2) The trenching depth corresponding to the changes of the nozzle diameters showed its maximum depth when the diameter was 3 m, and the trenching efficiency increased as the spray pressure increased as well.
- (3) For Type I in order to ensure the trenching depth required in actual operation, it is found that at least $3.0 \text{ m}^3/\text{h}$ of flow rate and 0.11 m/s of a trenching speed are necessary.
- (4) For Type II, it is found that trenching performance and working efficiency

decreases as the nozzle angle gets smaller and the advancing speed increases. In particular, when the angle of a nozzle to the seabed was 60 degree the trenching depth was difficult to measure at the speed of 0.11 m/s or more. Thus, it suggests that additional experiments are necessary to ensure the engineering reliability.

- (5) The maximum trenching depth measured in the model experiments was 2.78 m, which was very similar to the maximum depth of 3 m. Moreover, the flow rate used in the experiments was at about a 30% level when compared with that of machines currently in operation. Thus, it is found that when it operates at a 100% flow rate in actual waters, it can ensure superior trenching depth and speed, resulting in an increase in work efficiency.



References

- Adamson, J.E., Kollé, J.J., 1996. Development of a water jetting Cable Burial System for a Broad Range of Soils in up to 2500 Meters of Seawater. *Presentation at Underwater Intervention '96, Marine Technology Society.*
- ANSYS, Inc.,(2011), *ANSYS CFX-Solver Theory Guide*, Release 14.0
- Berghe, J.V., Capart, H. & Su, J.C.C., 2008. Jet Induced Trenching Operations : Mechanisms Involved. *Proceeding of 2008 Offshore Technology Conference, OTC(19441)*, USA.
- Berghe, J.V., Pyrah, J., Gooding, S. & Capart, H., 2011. Development of a Jet Trenching Model in Sand. *Frontiers in Offshore Geotechnics II*, 889-894.
- Canyon Helix Offshore 2013, T-1200 [Online] Available at : <http://helixesg.com/case-studies/t1200-windfarm-trenching-case-study/>
- Dansette, N., and Robertson, N. C., 1994. Subsea Flexible Pipeline Burial Using a Lightweight Pipeline Trencher. In *Offshore Technology Conference*, ISBN 978-1-61399-096-4
- Deep Ocean 2015, UT-1, [Online] Available at : <http://www.deepoceangroup.com/>
- Det Norske Veritas, 2007. On-Bottom Stability Design of Submarine Pipelines. *Det Norske Veritas (DNV)*, Oslo, Norway. DNV-RPF109
- Global Marine Systems 2015, Q-1000, [Online] Available at: <http://www.globalmarinesystems.com/subsea-equipment.html>
- Kim, H.A., 2006. *A Study on the Basic Design of Sub-sea Trenching Machine Using Water Jetting*. MSc thesis, Graduated Institute of Ocean system Engineering, Korea Maritime and Ocean University.
- Kozhevnickov, N. N., 2004. A Theory of Soil Ripping by a Submerged Water jet and

- the Design of Jet Soil Ripping for Dredgers, *Power Technology and Engineering*, Vol 38, No 3, 21-27
- Li, J.H. et al., 2014. Consideration on Optimal Construction of Thrust System for Improvement of ROV Trencher's Cable Burying Performance. *2014 29th ICROS Annual Conference*. 482-483
- Na, K. W. et al., 2015. A Fundamental Study to Estimate Construction Performance of Subsea Waterjet Trenching Machine. *Journal of Navigation and Port Research*, 39(6), pp. 539-544
- Na, K. W. et al., 2015. Study on Performance Evaluation of Subsea Waterjet trenching Machine Using Water Tank. *Journal of Ocean engineering and Technology*, 29(6), pp. 470-474
- O'Donoghue, T., Trajkovic, B. & Piggins, J., 2001. Sand Bed Response to Submerged Water Jet. *Proceeding of the Eleventh International Offshore and Polar Engineering Conference*. Stavanger Norway. 66-72.
- Perng, A.T.H., Capart, H., 2008. Underwater Sand Bed Erosion and Internal Jump Formation by Travelling Plane Jets. *Journal of Fluid Mechanics*, 595, 1-43.
- Seo, Y.K., Lee, K.Y., Ha, K.S. & Kim, T.H., 2012. Technical Articles: Geotechnical Aspects of Submarine Cable. *Korea Geotechnical Society*. 28(3) pp. 12-22
- Su, J.C.C., Perng A.T.H. & Capart. H., 2007. Underwater Trenching Incision and Turbid Overspill due to Moving Point Jets. *In Proceedings of the Congress-International Association for Research* 32(2), 544
- Tateyama, K. and Nishitani, M., 2000. Fundamental study on development of a new type of submarine cable layer. *Journal of civil engineering*, No. 658/VI-48, pp. 255-265